Journal of Neuroscience Methods 312 (2019) 37–42

Contents lists available at ScienceDirect

Journal of Neuroscience Methods

journal homepage: www.elsevier.com/locate/jneumeth

Variability and uncertainty in the rodent controlled cortical impact model of traumatic brain injury

Prabu Sellappan[a,1], Jason Cote[b,2], Phillip A. Kreth[a,3], Victor D. Schepkin[c,5], Ali Darkazalli[b,d], Deborah R. Morris[d], Farrukh S. Alvi[a,4], Cathy W. Levenson[b,d,*,6]

[a] Mechanical Engineering and Florida Center for Advanced Aero-Propulsion, FAMU-FSU College of Engineering, Tallahassee, FL, United States
[b] Program in Neuroscience, Florida State University, Tallahassee, FL, United States
[c] National High Magnetic Field Laboratory, Florida State University, Tallahassee, FL, United States
[d] Department of Biomedical Sciences, Florida State University College of Medicine, Tallahassee, FL, United States

ARTICLE INFO

Keywords:
TBI
Lesion
Injury
Impact
CCI

ABSTRACT

Background: Controlled cortical impact (CCI) has emerged as one of the most flexible and clinically applicable approaches for the induction of traumatic brain injury (TBI) in rodents and other species. Although this approach has been shown to model cognitive and functional outcomes associated with TBI in humans, recent work has shown that CCI is limited by excessive variability in lesion size despite attempts to control velocity, impact depth, and dwell time.

New method: Thus, this work used high-speed imaging to evaluate the delivery of cortical impact and permit the identification of specific parameters associated with technical variability in the CCI model.

Results: Variability is introduced by vertical oscillations that result in multiple impacts of varying depths, lateral movements after impact, and changes in velocity, particularly at the prescribed impact depth.

Conclusions: Together these data can inform future work to design modifications to commonly used CCI devices that produce TBI with less variability in severity and lesion size.

1. Introduction

Given the paucity of treatments for traumatic brain injury, consistent, reproducible animal models of TBI that produce both the short- and long-term outcomes associated with TBI in humans are essential. While there are a number of models that have been employed such as the fluid percussion injury (FPI) and weight drop models, controlled cortical impact (CCI) has emerged as one of the most flexible and clinically applicable approaches. There are a number of advantages to this model. First, it permits the induction of a wide range of injury severity including mild, moderate, and severe TBI, as well as, more recently, closed head mild and repetitive traumatic brain injury. The flexibility of the CCI model is also illustrated by the fact that it has been used in both rats and mice (Darkazalli et al., 2017; Zweckberger et al., 2003; Dixon et al., 1991), as well as ferrets (Lighthall, 1988), pigs of different ages (Hawryluk et al., 2016; Pareja et al., 2016), and non-

* Corresponding author.
E-mail addresses: psellappan@fsu.edu (P. Sellappan), jcote@neuro.fsu.edu (J. Cote), pkreth@utsi.edu (P.A. Kreth), schepkin@magnet.fsu.edu (V.D. Schepkin), falvi@fsu.edu (F.S. Alvi), cathy.levenson@med.fsu.edu (C.W. Levenson).
[1] Complete Address: Prabu Sellappan, Aero-Propulsion, Mechatronics and Energy Building, Florida State University, 2003 Levy Ave, Tallahassee, FL, 32310. Tel.: 850-645-2634; Fax: 850-645-0112.
[2] Complete Address: Jason Cote, Department of Biomedical Sciences, Florida State University College of Medicine, 1115 W. Call St., Tallahassee, FL, 32306. Tel.: 813-381-0056; Fax: 850-644-5781.
[3] Current Address: Phillip A. Kreth, Department of Mechanical, Aerospace, and Biomedical Engineering, The University of Tennessee Space Institute, 411 B.H. Goethert Parkway, MS-18, Tullahoma, TN. Tel.: 931-393-7484.
[4] Farrukh S. Alvi, Aero-Propulsion, Mechatronics and Energy Building, Florida State University, 2003 Levy Ave, Tallahassee, FL, 32310. Tel.: 850-645-2634; Fax: 850-645-0112.
[5] Complete Address: Victor D. Schepkin, National High Magnetic Field Laboratory, 1800 E. Paul Dirac Dr. Tallahassee, FL, 32310. Tel.: 850-645-7357; Fax: 850-644-1366.
[6] Complete Address: Cathy W. Levenson, Department of Biomedical Sciences, Florida State University College of Medicine, 1115 W. Call St., Tallahassee, FL, 32306. Tel.: 850-212-0191; Fax: 850-644-5781.

https://doi.org/10.1016/j.jneumeth.2018.10.027
Received 3 September 2018; Received in revised form 8 October 2018; Accepted 17 October 2018
Available online 10 November 2018

human primates (King et al., 2010).

Outcomes associated with TBI induced by CCI are consistent with those associated with brain injury in humans (Brody et al., 2007; Turtzo et al., 2013; Romine et al., 2014; Marklund, 2016). Functional and cognitive deficits associated with CCI model human TBI and include deficits in spatial learning and memory (Cope et al., 2012, 2011), recognition memory (Darkazalli et al., 2016), and a variety of motor functions (Brody et al., 2007). Limbic and frontal lobe functions are also modeled well by CCI, with rodents exhibiting depression-like, and anxiety-like behaviors (Cope et al., 2011; Darkazalli et al., 2016) Histologically, CCI has been shown to produce many relevant pathophysiological changes including primary and secondary neuronal death (Newcomb et al., 1999), changes in hippocampal and subventricular zone cell proliferation (Darkazalli et al., 2016; Cope et al., 2016; Chang et al., 2016), disruption of the blood-brain-barrier (Glushakova et al., 2014), and evidence of oxidative stress and inflammation (Chen et al., 2017; Harting et al., 2008). Together these features make CCI an attractive model for evaluating the effects of TBI over time and for use in testing the efficacy of new therapeutic agents.

Much of the flexibility and usefulness of this method is derived from the ability to control the size of the impact, the shape and material of the impact piston, and the placement of the injury, as well as the type of anesthesia and replacement (or not) of the bone flap removed during craniotomy prior to injury. The severity of the injury is also controlled by changes in contusion depth, impact velocity, and dwell time. While providing flexibility, induction of TBI by CCI is also known to be limited by significant variability in the injury. While most studies have not rigorously reported how consistent the injuries produced were, recent reports using MRI to evaluate injury suggest that technical variability associated with CCI devices is likely to be greater than previously appreciated and even exceed normal biological variability (Turtzo et al., 2013). Thus, this work sought to use high-speed imaging to evaluate the impact process and enable us to identify specific parameters associated with technical variability in the CCI model.

2. Materials and methods

2.1. Controlled cortical impact

The CCI was produced by investigators with approximately 5 years of experience using the Impact One stereotaxic impactor for CCI (Leica Biosystems, Buffalo Grove, IL) (Darkazalli et al., 2017, 2016; Cope et al., 2016). The apparatus was fitted to a Kopf small animal stereotaxic frame (model 940) equipped with 10 μm resolution digital display. Impact parameters, consistent with previously published reports using this approach to model human TBI in rodents, were controlled to 2.25 m/s impact velocity, a depth of 3.0 mm, and a dwell time of 500 ms as previously described (Darkazalli et al., 2017; Cope et al., 2012; Darkazalli et al., 2016; Cope et al., 2016). All procedures were carried out using aseptic techniques and in accordance with institutional animal care and use guidelines. Eight-week old male Sprague-Dawley rats were anesthetized with 2.5–3% isoflurane in oxygen. Body temperature was maintained using a heat pad and warm water-circulating system. Anesthetized rats were fixed into a stereotaxic frame and, following a 15 mm midline incision over the cranium, a 6 mm diameter midline craniotomy was performed immediately rostral to bregma. The CCI device was then used to deliver a 5 mm diameter bilateral cortical injury as previously described (Darkazalli et al., 2017; Cope et al., 2011, 2012; Darkazalli et al., 2016; Cope et al., 2016). Subject to all NIH guidelines, the animal procedures were approved by the Institutional Animal Care and Use Committee (IACUC).

2.2. Magnetic resonance imaging (MRI)

Diffusion weighted magnetic resonance images (MRI) were acquired 8 days after implementing TBI procedures (n = 5). Images were acquired using the 900 MHz, 21.1 T MRI scanner equipped with Bruker Avance III console, PV5.1 software at the National High Magnetic Field Laboratory on the campus of Florida State University. The *in vivo* MRI probe had volume RF coil with diameter of 33 mm, which was able to accommodate a rat head. Animals were kept inside the RF coil *via* a bite bar with continuous delivery of the inhalant anesthesia, isoflurane (2%). The temperature inside the magnet bore was controlled to 30 °C. The diffusion spin-echo pulse sequence had 3D diffusion gradients, echo time TE = 34 ms, and diffusion weighting factor b = 100 s/mm (Zweckberger et al., 2003). Fifteen slices were acquired using the imaging matrix of 128 × 128, slice thickness of 0.7 mm and a slice gap of 0.3 mm. The repetition time of the diffusion scan was 3.75 s and the total duration of the MRI scan time was 16 min Schepkin et al. (2012). Volumetric analysis of the lesion was performed using AMIRA 4.0.2 (FEI, Hillsborough, OR) and reported as mm (Dixon et al., 1991). The edge of injury as visualized in the 3D GRE scan and traced. The TBI was then segmented manually as previously described (Darkazalli et al., 2016).

2.3. Impact imaging

After craniotomy, CCI was evaluated using a high-speed CMOS camera (Phantom v411 Digital High Speed Camera) and Phantom Camera Control software from Vision Research (n = 9). High-speed camera images were recorded with timing accuracy of 20 ns and bit-depth of 8 bits per pixel. Impactor motion was captured both with and without a rat present in the stereotaxic frame under the same conditions. For all *in vivo* trials images were recorded at a frame rate of 8000 frames/s, image resolution of 800 × 400 pixels and 0.16 mm/pixel spatial resolution (representative video shown in Supplemental Material 3). The camera was positioned above the horizontal plane of the craniotomy to allow for a field of view (FOV) that includes the impactor at initial position and the craniotomy itself (Supplemental Material 1). Additional runs were recorded in the stereotaxic device prior to animal placement at 5000 FPS, with a superior image resolution of 1280 × 304 pixels and spatial resolution of 0.02 mm/pixel to assess the impactor's full range of motion (representative video shown in Supplemental Material 4).

2.4. Image processing

Images were processed using custom MATLAB codes (source code included as Supplemental Material 2), based on the normalized 2D cross-correlation routine available through the MATLAB Image Processing Toolbox. Each data set contained a time series of images capturing the impactor motion from its initial position through impact and dwell. Impactor motion was tracked and measured using a multi-step pattern recognition algorithm, described herein. A sub-region within the first image in the time-series was manually selected. This image template was selected to encompass an appropriate region of the first image, such as, regions of the impactor with banded markings, or in the cases without animal placement in the stereotaxic device, the tip of the impactor. The normalized 2D cross-correlation of the selected image template and the second image in the time series was then calculated, and the peak in the cross-correlation matrix identified. The location of the peak indicates the most probable location of the selected template pattern in the second image, and is therefore a measure of the displacement of the impactor during the time interval between recordings of the two images. This procedure was repeated for subsequent images in the time-series, with the template being updated after every iteration to account for changes in luminance in the image as the impactor moves. This pattern recognition technique is quite robust, and can effectively pattern match the selected template to the corresponding scene in the next image with high accuracy, especially in regions with good image texture and high spatial resolution. The position of the template in each matched image was recorded, and based

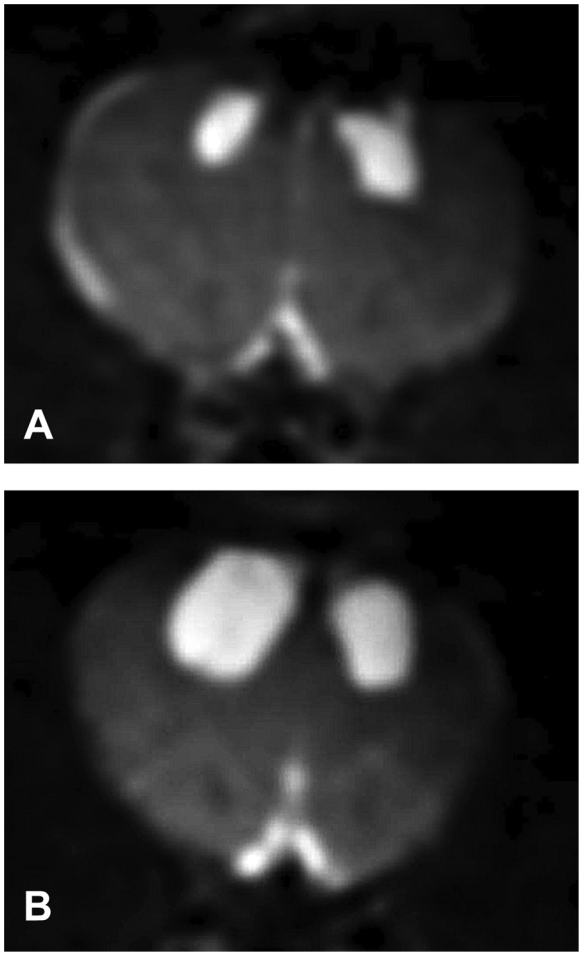

Fig. 1. Diffusion weighted MR images from two rats 8 days after traumatic brain injury by CCI showing the range of the variability of injury. The large white cortical areas represent extent of brain damage and illustrate the large variation in lesion volume for the matching positions of the rat brain. Image (A) shows damage volume of 6.3 mm (Dixon et al., 1991) and image (B) illustrates damage volume of 27.5 mm (Dixon et al., 1991).

on template position, image acquisition frame rate, and spatial resolution, the position (vertical and lateral) of the impactor was calculated. The velocity of the impactor was then calculated from the position (displacement) and frame rate (temporal information) using a central differencing scheme. The accuracy and effectiveness of this motion tracking technique was validated using a capacitive displacement sensor (C1-A Probe coupled to CPL290 Driver from Lion Precision) with a measurement resolution of 30 nm.

3. Results

3.1. In vivo injury variability

Although all variables were held constant, there was significant variation in the size of the lesion 8 days post-TBI. The lesion volume for all animals analyzed was 16.2 ± 8.0 mm (Dixon et al., 1991) (mean ± SD). Fig. 1 shows the two animals with the largest discrepancy in lesion volume.

3.2. Image tracking technique validation

The position of the impactor, calculated using the image tracking technique, was compared with the position measured by the capacitive sensor prior to the animal being fixed into the stereotaxic device. Fig. 2 shows the mean impactor position during test runs (n = 10) of impactor movement calculated using the image-based tracking method described above, along with data from the capacitive sensor. Within the maximum detection range (2 mm) of the capacitive displacement sensor there was a high level of correlation between the mean impactor positions measured by the two independent measurement techniques.

3.3. Evaluation of variability during CCI

High-speed imaging revealed the impactor bounce back up after the initial cortical impact in the *in vivo* model of CCI. Additionally, there were multiple secondary impacts before the piston reached its final impact depth. This motion occurred within < 10 ms following initial impact.

Fig. 3 shows the impactor position as a function of time from its initial position until it stabilized at the specified 3 mm impact depth (open circles). The variability associated with these vertical movements is shown by the error bars (-1.24 ± 2.09 mm at time 0.0050 s). Fig. 4 shows the corresponding mean velocity profile (-0.25 ± 1.61 m/s at time step when the impactor piston reached impact depth of 3 mm and -2.39 ± 0.72 m/s at time step when the impactor piston reached full depth) of the piston before and after cortical impact as well as the significant variability associated with this parameter. The velocity profile indicates negative velocity (downward motion) initially, but after impact the velocities become positive, indicating reversed, upward motion before reversing again with subsequent impacts. These secondary impacts have progressively lower velocities and after third impact the amplitude of impactor velocity becomes insignificant and falls below the measurement threshold.

3.4. Evaluation of variability during simulated CCI

To fully characterize the impactor motion, experiments were also performed by simulating CCI to provide unobstructed optical access over the full range of motion of the impactor piston and at a higher spatial resolution, allowing higher accuracy in motion tracking. Fig. 3 shows the position of the impactor (solid line) under simulated conditions with variability and uncertainty (shaded region). The mean velocity profile for the same data set, calculated from the position data, is shown in Fig. 5, along with its uncertainty. Impactor velocity at depth equivalent to depth of tissue impact was -2.44 ± 0.16 m/s and at depth equivalent to prescribed impact depth was -2.34 ± 1.38 m/s.

In addition to vertical movements of the piston, the higher spatial resolution of simulated measurements also made it possible to detect and evaluate the lateral position of the impactor piston during CCI. Fig. 6 shows the lateral deviations of impactor from the centerline as it moves down toward the impact position. Of note is not only the significant variabilty in this motion, but also the observation that a majority of the lateral movement is in one direction (right) from midline with a mean maximum deviation of 0.76 ± 0.16 mm.

4. Discussion

MR imaging of rats one week post-TBI to examine showed that the variability in lesion volume produced by CCI was comparable to previous reports in the literature. (Turtzo et al., 2013) The finding that magnitude of this variability can exceed biological variability limits the usefulness of this method, particularly when examining treatments that are expected to produce real, but small, improvements. Thus, this work sought to determine the sources of variability with the goal of informing modifications to the method and equipment to reduce variation in injury size and severity.

To do this we used high speed camera images to evaluate CCI after craniotomy in the rat model as well as in a simulated CCI procedure that permitted higher resolution imaging coupled with inherently superior optical access. Comparison of *in vivo* and simulated motion

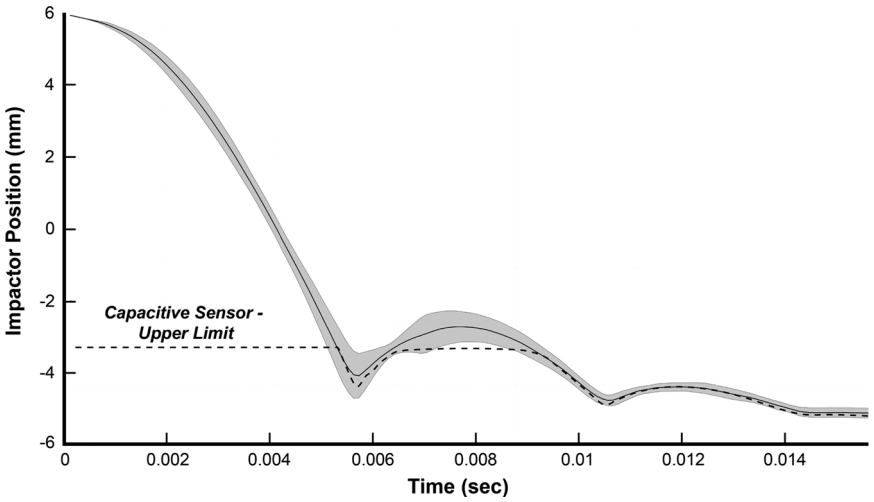

Fig. 2. Mean impactor position simultaneously measured through image pattern recognition (motion tracking) and capacitive sensing. Solid line – motion tracking; dashed line – capacitive sensing. Shaded region indicates uncertainty of ± SD; N = 10.

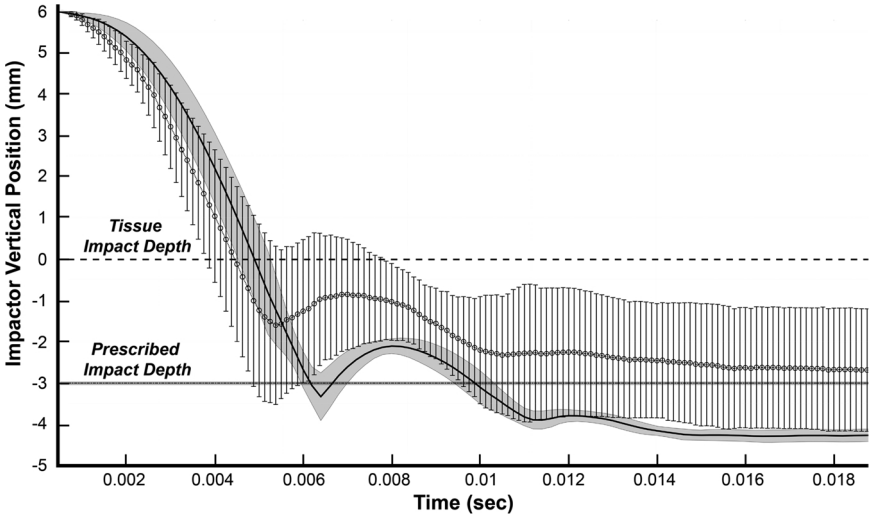

Fig. 3. Impactor position over time indicating multiple impacts. Dashed line with circle markers – impactor mean position with rat present in stereotax; Thick, solid line – impactor mean position without rat present. N = 9; Shaded region and error bars indicate uncertainty of ± SD.

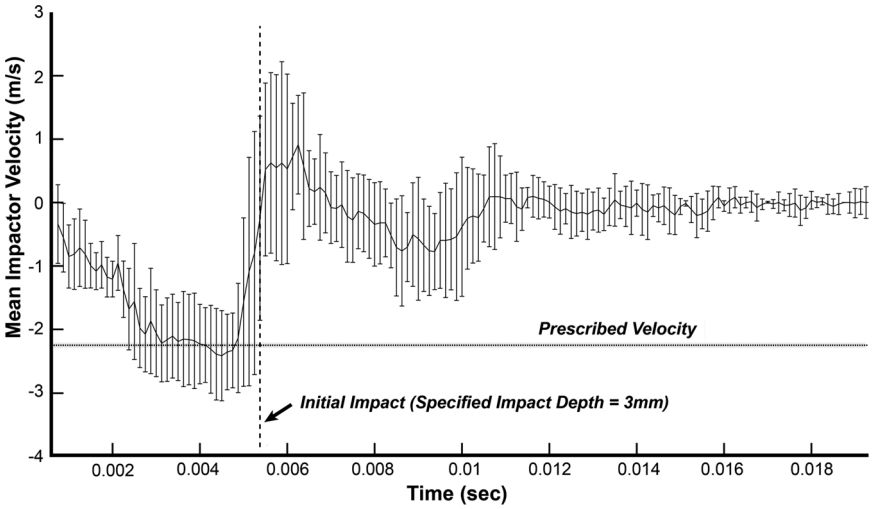

Fig. 4. Impactor velocity profile in the presence of rat in stereotaxic frame. Solid line indicates mean velocity; error bars indicate uncertainty of ± SD; N = 9.

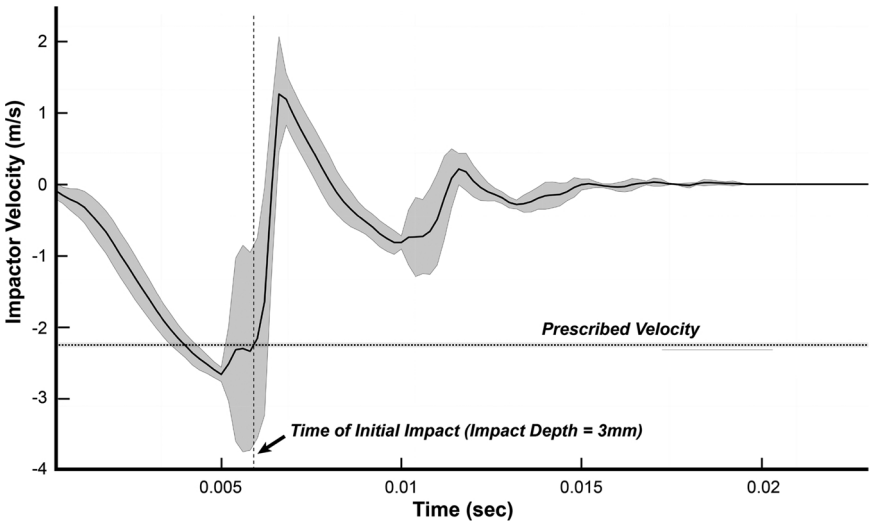

Fig. 5. Velocity profile of impactor in the absence of rat in stereotaxic frame. Solid line indicates mean velocity; shaded region indicates uncertainty of ± SD; N = 9.

profiles showed that the measured position in both cases, especially in the initial descent stage, coincide with in measurement uncertainty such that both profiles were qualitatively similar. It was, therefore, quite reasonable to simulate the impactor motion and derive meaningful data that could be applicable to the use of CCI in a rodent model. An advantage of this approach is that any movements in the piston originating from the stereotaxic arm were included in the imaging and thus in the calculations of variability and uncertainty.

In both the rat model and the simulated impact the motion profile indicated that the impactor reached the preset impact depth, but subsequently underwent at least three vertical oscillations before finally stabilizing at a depth that was lower than the prescribed value. These oscillations, which produced additional impacts, were not influenced by dwell time because the oscillations were complete and the piston was at rest in less than 10 ms and the lowest dwell time on many commercially available devices is 100 ms. Because each of these oscilations occurred below the impact point on the brain, these additional impacts contribute to the severity of the injury. The velocity profile indicated that while the impactor traveled faster than the prescribed velocity before it reaches impact depth, at cortical impact the mean velocity was found to be nominally equal to the preset velocity. This suggests that the equipment was performing as designed at impact. However, the higher velocities and large variance immediately before impact were unexpected. The relatively high variance in velocity at the prescribed impact depth is caused by rapid deceleration of the impactor once it overshoots prescribed velocity. Together these data suggest that changes in velocity and the accompanying variation in velocity contribute significantly to obseved variations in tissue damage.

It is worthwhile to note that lateral movements of the piston are also present. These observed movements would clearly be expected to affect the force imparted onto the cortical tissue. Results showing the magnitude of lateral motion indicate the lateral deviation is initially minimal, but increases during the latter stages of motion. In the simulated CCI model the mean lateral deviaton (0.7 mm) exceeded the available space (0.5 mm) between the skull and the 5 mm diameter piston placed inside a 6 mm craniotomy. The direction of the lateral movements in the plane measured was consistently in the same direction, consistent with the fact that the piston is screwed into the impact device. The lateral devations are constrained by the skull. However, this suggests the likely occurance of multiple secondary impacts on the skull and additonal glancing impacts, all causing variabilty in injury severity. A limitation of this work is that we report lateral movement from only a single plane. Lateral movements of the piston after tissue impact along all planes clearly increase the number of potential secondary impacts.

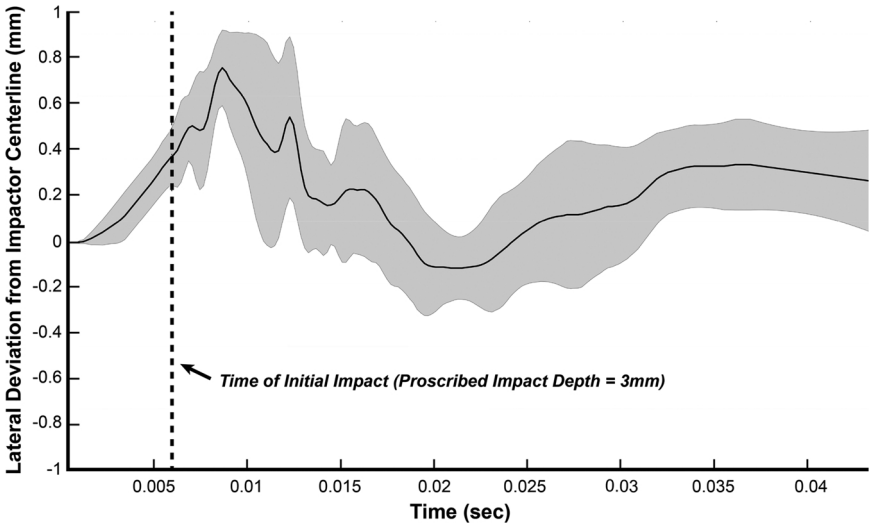

Fig. 6. Lateral deviation of impactor position in the absence of rat in stereotaxic frame. Solid line indicates mean lateral position of impactor with respect to impactor centerline axis at start. Shaded region indicates uncertainty of ± SD; N = 9.

Thus, while the distance of the lateral deviations are expected to be significanltly reduced by the immobile skull when the animal is fixed securely in the stereotaxic frame, this comes at the cost of increased tissue damage and variability of injury severity.

5. Conclusions

In conclusion, this work has shown that although the CCI method is designed to deliver a single, controlled impact to the cortex after crainotomy, variablity is introduced by the occurance of multiple impacts. We also report significant variations in velocity, particularly at the point of prescribed contusion depth. Finally, we observed significant lateral movements in the piston occuring during and after impact that contribute to uncertainty in the method. Although only one type of CCI device was tested (electromagnetic), the work reported here suggests that other models would have similar issues as both variability and uncertainty would be common to all electromagnetically driven pistons. These findings can be used to inform future work to modify CCI devices that produce TBI with less variability in severity and lesion size. It is known from classical Newtonian mechanics that higher velocity necessarily leads to higher kinetic energy for a given mass of impactor, and results in more potent secondary impacts which will increase injury variability. Specifically, this work suggests that to reduce variability the lowest possible velocity needed to achieve the desired behavioral, cellular, or molecular outcomes should be employed. Additionally, the length of commercially available pistons varies greatly. Use of shorter pistons is recommended as increased piston length will magnify lateral displacement observed in this work and increase variability of piston motion. The ratio of craniotomy size to impactor diameter should be considered to prevent secondary impacts on the skull due to lateral movements of the piston. Thus, this work has identified sources of variability and uncertainty that can serve as the basis for future design improvements that produce more reliable data.

Acknowledgements

This study was partially performed at the National High Magnetic Field Laboratory (Tallahassee) supported by NSF Grant No. DMR 11549.

Conflict of interest statement

The authors have no competing financial interests.

Appendix A. Supplementary data

Supplementary material related to this article can be found, in the online version, at doi:https://doi.org/10.1016/j.jneumeth.2018.10.027.

References

Brody, D.L., Mac Donald, C., Kessens, C.C., Yuede, C., Parsadanian, M., Spinner, M., Kim, E., Schwetye, K.E., Holtzman, D.M., Bayly, P.V., 2007. Electromagnetic controlled cortical impact device for precise, graded experimental traumatic brain injury. J. Neurotrauma 24, 657–673.

Chang, E.H., Adorjan, I., Mundim, M.V., Sun, B., Dizon, M.L., Szele, F.G., 2016. Traumatic brain injury activation of the adult subventricular zone neurogenic niche. Front. Neurosci. 10, 332.

Chen, W., Guo, Y., Yang, W., Zheng, P., Zeng, J., Tong, W., 2017. Connexin40 correlates with oxidative stress in brains of traumatic brain injury rats. Restor. Neurol. Neurosci. 35, 217–224.

Cope, E.C., Morris, D.R., Scrimgeour, A.G., VanLandingham, J.W., Levenson, C.W., 2011. Zinc supplementation provides behavioral resiliency in a rat model of traumatic brain injury. Physiol. Behav. 104, 942–947.

Cope, E.C., Morris, D.R., Scrimgeour, A.G., Levenson, C.W., 2012. Use of zinc as a treatment for traumatic brain injury in the rat: effects on cognitive and behavioral outcomes. Neurorehabil. Neural Repair 26, 907–913.

Cope, E.C., Morris, D.R., Gower-Winter, S.D., Brownstein, N.C., Levenson, C.W., 2016. Effect of zinc supplementation on neuronal precursor proliferation in the rat hippocampus after traumatic brain injury. Exp. Neurol. 279, 96–103.

Darkazalli, A., Ismail, A.A., Abad, N., Grant, S.C., Levenson, C.W., 2016. Use of human mesenchymal stem cell treatment to prevent anhedonia in a rat model of traumatic brain injury. Restor. Neurol. Neurosci. 34, 433–441.

Darkazalli, A., Vied, C., Badger, C.D., Levenson, C.W., 2017. Human mesenchymal stem cell treatment normalizes cortical gene expression after traumatic brain injury. J. Neurotrauma 34, 204–212.

Dixon, C.E., Clifton, G.L., Lighthall, J.W., Yaghmai, A.A., Hayes, R.L., 1991. A controlled cortical impact model of traumatic brain injury in the rat. J. Neurosci. Methods 39, 253–262.

Glushakova, O.Y., Johnson, D., Hayes, R.L., 2014. Delayed increases in microvascular pathology after experimental traumatic brain injury are associated with prolonged inflammation, blood-brain barrier disruption, and progressive white matter damage. J. Neurotrauma 31, 1180–1193.

Harting, M.T., Jimenez, F., Adams, S.D., Mercer, D.W., Cox, C.S.Jr., 2008. Acute, regional inflammatory response after traumatic brain injury: implications for cellular therapy. Surgery 144, 803–813.

Hawryluk, G.W., Phan, N., Ferguson, A.R., Morabito, D., Derugin, N., Stewart, C.L., Knudson, M.M., Manley, G., Rosenthal, G., 2016. Brain tissue oxygen tension and its response to physiological manipulations: influence of distance from injury site in a swine model of traumatic brain injury. J. Neurosurg. 125, 1217–1228.

King, C., Robinson, T., Dixon, C.E., Rao, G.R., Larnard, D., Nemoto, C.E., 2010. Brain temperature profiles during epidural cooling with the ChillerPad in a monkey model of traumatic brain injury. J. Neurotrauma 27, 1895–1903.

Lighthall, J.W., 1988. Controlled cortical impact: a new experimental brain injury model. J. Neurotrauma 5, 1–15.

Marklund, N., 2016. Rodent models of traumatic brain injury: methods and challenges. Methods Mol. Biol. 1462, 29–46.

Newcomb, J.K., Zhao, X., Pike, B.R., Hayes, R.L., 1999. Temporal profile of apoptotic-like changes in neurons and astrocytes following controlled cortical impact injury in the rat. Exp. Neurol. 158, 76–88.

Pareja, J.C., Keeley, K., Duhaime, A.C., Dodge, C.P., 2016. Modeling pediatric brain trauma: piglet model of controlled cortical impact. Methods Mol. Biol. 1462, 345–356.

Romine, J., Gao, X., Chen, J., 2014. Controlled cortical impact model for traumatic brain injury. J. Vis. Exp. 5, e51781.

Schepkin, V.D., Bejarano, F.C., Morgan, T., Gower-Winter, S.D., Ozambela, M.Jr., Levenson, C.W., 2012. In vivo magnetic resonance imaging of sodium and diffusion in rat glioma at 21.1 T. Magn. Reson. Med. 67, 1159–1166.

Turtzo, L.C., Budde, M.D., Gold, E.M., Lewis, B.K., Janes, L., Yarnell, A., Grunberg, N.E., Watson, W., Frank, J.A., 2013. The evolution of traumatic brain injury in a rat focal contusion model. NMR Biomed. 26, 468–479.

Zweckberger, K., Stoffel, M., Baethmann, A., Plesnila, N., 2003. Effect of decompression craniotomy on increase of contusion volume and functional outcome after controlled cortical impact in mice. J. Neurotrauma 20, 1307–1314.